Indian Journal of Chemical Technology
Vol. 24, May 2017, pp. 284-293

Nano $Fe(OH)_3$/zeolite as a novel, green and recyclable adsorbent for efficient removal of toxic phosphate from water

Azadeh Mikhak[1], Mohammad Zaman Kassaee*[,2], Akbar Sohrabi[1] & Mohammad Feizian[1]

[1]Department of Soil Science, Lorestan University, P.O. Box 68151-44316, Khoram Abad, Iran

[2]Department of Chemistry, Tarbiat Modares University, P.O. Box 14155-175, Tehran, Iran

E-mail: kassaeem@modares.ac.ir

Received 5 November 2015; accepted 18 October 2016

Magnetic $Fe(OH)_3$ is dispersed and stabilized over zeolite, giving rise to nano $Fe(OH)_3$/zeolite, which is used as an efficient, recyclable absorbent for phosphate removal from water. Phosphate removal is insensitive to the ionic concentration, yet is directly proportional with the concentration of the adsorbent, and is inversely proportional with the initial phosphate concentration and *p*H. The coexisting nitrate and bicarbonate anions have no significant influence on phosphate adsorption, while the presence of citrate or silicate decreases such adsorption. In contrast, the presence of acetate increases the phosphate removal. Kinetic data are well fitted in the pseudo-second-order model. High phosphate uptake capability and good reusability make $Fe(OH)_3$/Zeolite a potentially attractive adsorbent for the removal of toxic phosphate from water. Evidently this type of work is a step forward for large scale elimination of undesired contaminants from water which may benefit the world community.

Keywords: Phosphate, Zeolite, Water treatment, Nano iron hydroxide, Adsorption, Contaminant

The use of chemical fertilizers has been the only important factor in the rise of the world agricultural production in the past three decades[1]. In 2013, the global demand for macro elements such as nitrogen, phosphorus and potassium were 140, 48.9 and 42.7 million tons, respectively[2]. The total demand for nutrients was anticipated to increase from 217 to 236 million tons between 2012 and 2016. Fertilizers are used to increase the yield, but their excessive use has led to pollution of water and environmental resources[3]. Among fertilizers, those of nitrogen and phosphorus are used more frequently. Nevertheless, their high concentrations, often leads to eutrophication of surface water, wetlands, rivers, lakes, and reservoirs worldwide[4-6]. Important eutrophication indicators include: high growth of algae (phytoplankton), decrease of water quality and change in its odour and taste[7]. Excessive amounts of pollutants in the soil and water have been observed in areas with rapid population growth and economic development such as the United States[8], China[9,10] and Europe[11-13]. Agricultural activities, waste waters, industrial waste, and weathering of rocks are the main pathways of phosphate entrance in soil and water resources[14]. Yet, many believe agriculture is the major source of pollution[15]. Indiscriminate use of phosphorus fertilizers, not only decreases the yield, but disrupts the plant nutrition and lowers adsorption of microelements (Fe, Cu, and Zn), and finally leads to negative long-term impacts[16]. Intensive cultivation and excessive use of phosphorus fertilizers in Iran, has increased its pollution in soil and water resources in different areas of the country[17]. Phosphorus fertilizers may have high cadmium concentrations witch prevent adsorptions of some microelements[18]. To create eutrophication, only 0.005 to 0.05 mg/L phosphorous or 0.02 mg/L phosphorus is required[19]. Phosphate standard for drinking water and waste water discharge are 0.2 and 6 mg/L, respectively[20,21]. Conventional methods for removing phosphorus from waste water or polluted water are chemical and biological methods. Disadvantages of chemical methods include employment of expensive chemicals, sludge production, hard dehydration and low efficiency. Disadvantages of biological systems include difficulty in controlling the process inefficiency[22,23]. Using nanoparticles is an effective approach to environmental recovery. It has applications in sewage treatment and solutions for soil contaminations. This method is fast, easy and cost effective[24]. Nanoparticles are very diverse. They include zero valent iron nanoparticles (Fe NPs) that are non-toxic, insoluble and due to their

small size, specific surface area and high reactivity are used for *in situ* applications[25-27]. Despite for Fe NPs benefits, they show some persistence during the reaction[28]. They rapidly oxidize when exposed to air[29]. So far, several studies have been done on phosphate removal. About 13.65 mg/g P was removed at *p*H = 4, *via* Fe-Zr magnetic oxide[30]. In another study, iron-titanium oxide nanoparticles were used for phosphate removal[31]. In addition, nanostructured Fe-Cu oxide was used for removing excess phosphate from water[32]. The efficiency of nanoparticles is gradually diminished. The important factor affecting nanoparticles efficiency is their possible aggregation during synthesis which leads to a decrease in their active surface area. So far, various methods have been used to overcome this problem, including the use of stabilizers[33,34]. Silicone stabilizers associated with Cu, Ni, Fe nanoparticles have been employed[35]. Activated carbon was also used for creation of stability[36]. Iron and manganese oxide nanoparticles stabilized on carboxymethyl cellulose (CMC) was used to adsorb As(V) and As(III) from water[37]. Nitrate removal was enhanced *via* graphene oxide coated Fe, Ni and Co nanoparticles[38]. Saturated zeolite with sodium and iron nanoparticles was used for phosphate removal from runoff[39]. Nanoparticles (TiO_2, Al_2O_3, Fe_2O_3) were able to remove phosphate from the solution, where the removal rate decreased with increasing *p*H[40]. Fe NPs stabilized on grapheme were also able to remove phosphate from a solution[41]. In addition sand particles were also employed as stabilizers for elimination of phosphate and arsenic[42]. Stabilization of iron nanoparticles could speed up and increase the efficiency of elimination[43]. In this paper we have used zeolite as a stabilizer form an iron hydroxide and have measured its ability for phosphate removal in comparison with neat Fe NPs.

Experimental Section

Materials

Fe NPs and nano Fe(OH)$_3$/Zeolite are two adsorbents that were used here for removal of phosphate.

Synthesis of Fe NPs

5.0 g of $FeSO_4 \cdot 7H_2O$ (98%, Aldrich) was dissolved in 250 mL of 30% technical grade methanol and 70% deionized water (v/v). The *p*H was adjusted to about 6.8 by 3M NaOH. Then 2.0 g of $NaBH_4$ powder (98%, Aldrich) was dissolved in 10 mL deionized water and the solution was added gradually to the mixture, allowing the foaming to subside between increments which finally resulted in ferric ion (Fe^{3+}) reduction Eq. (1). After addition of all of the $NaBH_4$ solution, the mixture was stirred for 45 min and then centrifuged for another 15 min at 5000 rpm. The solid was washed twice with technical grade methanol. The resulting solid was dried for 6 h under N_2 atmosphere and then broken up with a spatula to form a fine black powder[44,45].

$$Fe(H_2O)_6^{3+} + 3BH_4^- + 3H_2O \rightarrow Fe^0\downarrow + 3B(OH)_3 + 10.5H_2 \quad \ldots (1)$$

Synthesis of nano Fe(OH)$_3$/Zeolite

5.0 g of $FeSO_4 \cdot 7H_2O$ (98%, Aldrich) was dissolved in 250 mL of 30% technical grade methanol and 70% deionized water (v/v). Then 1.0 g zeolite was added and shaked for 60 min. Natural zeolite was collected from a mine in Semnan province, central Iran. It was used as a stabilizer for the Fe nanoparticles and was grounded to a size of 0.5 - 1mm. The *p*H was adjusted to 6.8 by 3M NaOH. The mixture was stirred for 20 min and then centrifuged for another 15 min, at 5000 rpm. The solid was washed twice with technical grade methanol. The resulting solid was dried and then broken up with a spatula to form a fine black powder.

Characterization of the nanoparticles

The particle size and morphology were investigated by PHILIPS (EM208S, the Netherlands) transmission electron microscopy (TEM) at 100 kV of acceleration voltage and scanning electron microscopy (SEM) of a Holland Philips EM3200 microscope with an accelerating voltage of 26 kV. Crystal structures were examined by using a Holland Philips Xpert X-ray powder diffraction (XRD) diffractometer (Cu K, radiation, λ= 0.154056 nm).

Phosphate removal experiments

Stock solution of P (1000 mg/L) was prepared by dissolving suitable amounts of KH_2PO_4 in deionized water. Phosphate removal was affected by different conditions such as adsorbents dosage, *p*H, initial phosphate concentration and sorption time. Batch experiments were carried out in 50 mL polyethylene bottles with either 0.02 g and 0.04 g of adsorbent (Fe NPs and nano Fe(OH)$_3$/Zeolite). Ten initial phosphate solutions concentrations were employed: 0, 5, 10, 15, 20, 25, 30, 35, 40, and 45 mg/L. Three ionic strengths for the solutions were adjusted by KCl (0.1, 0.01, 0.001 mol/ L). The *p*H was set at 2, 4, 6, 8, 10 and 12 using 0.1M HCl or NaOH. All bottles were shaken for 8 h and then centrifuged (4000, 20 min).

Phosphate concentration in supernatant was measured by UV-visible spectrophotometer (Varian model).

The sorption percent (%) of phosphate from solutions were calculated as Eq (2):

$$Sorption\ (\%) = \frac{C_0 - C_e}{C_0} 100 \quad \ldots (2)$$

where C_0 and C_e are the concentration of initial P and equilibrium time (mg/L), respectively. The sorption capacity (q_e, mg/g) of P were calculated using the following Eq (3):

$$q_e = \frac{(C_0 - C_e) V}{m} \quad \ldots (3)$$

where V and m are the volume of the solution (L) and mass of dry adsorbent (g), respectively. Each treatment was repeated thrice and the average concentrations were calculated from the replicate samples. Meanwhile, control experiments were also performed to exclude sorption of the P on the walls of the tubes.

Equilibrium time

The removal of phosphate by both nanoparticles (Fe NPs and nano $Fe(OH)_3$/ zeolite) was investigated at different time intervals (2, 4, 6, 8, 12, 24, 48 hours), with initial phosphate concentration of 15 mg/L. These experiments were carried out at *p*H = 2 in polyethylene bottles which included 40 mL of mono potassium phosphate (KH_2PO_4), solution and 0.04 g of either nano $Fe(OH)_3$/ zeolite or Fe NPs. Ionic strengths of 0.01 M KCl was used. After shaking each bottle for a defined time and centrifuging (4000 rpm, 20 min), the amount of phosphate was determined by a spectrophotometer.

Effects of adsorbent concentrations

Various concentrations of our synthesized nano materials were used to remove phosphate from aqueous solutions. Several initial concentrations of aqueous phosphate were treated with either 0.02 or 0.04 g of either Fe NPs or nano $Fe(OH)_3$\zeolite. Tests were carried out in 50 mL polyethelene bottles at *p*H = 2 and initial phosphate concentrations of 5, 10, 15, 20, 25, 30, 35, 40, and 45 mg/L.

Effects of *p*H on phosphate removal

Solutions containing various phosphate concentrations (5, 10, 15, 20, 25 mg/L) were prepared using KH_2PO_4. To the latter was added either 0.04 g of Fe NPs or the same amount of nano $Fe(OH)_3$\zeolite. Resultants were divided into 40 mL aliquots that were poured into 50 mL polyethylene bottles. Using 0.1 M HCl or NaOH, *p*H levels were adjusted to 2, 4, 6, 8, 10 and 12. Bottles were shaken for 8 h and then centrifuged (4000 rpm, 20 min) at 25 ± 1°C. The concentrations of phosphate in supernatant were measured by a UV-visible spectrophotometer.

Effects of ionic strength on phosphate removal

Removal of different concentrations of phosphate (5, 10, 15, 20, 25 mg/L) were investigated at *p*H = 2 using 0.04 g of adsorbent, at a variety of ionic strengths (0.1, 0.01, 0.001 M) adjusted by KCl.

Effects of coexisting anion

The effects of nitrate, bicarbonate, SiO_3, citrate and acetic on the phosphate removal were investigated by adding 0.01 M, $NaNO_3$, $NaHCO_3$, $NaSiO_3$, sodium citrate and sodium acetic to 10 mg/L phosphate solution, respectively. The *p*H was adjusted to 2.0±0.1. 0.04 g of nano $Fe(OH)_3$/Zeolite was added in each bottles that were mixed at 4000 rpm for 8 h at 25 ± 1°C. After 15 min centrifuged phosphate concentrations were analyzed.

Desorption test

Adsorption and desorption tests were carried out to evaluate their usability of the nano $Fe(OH)_3$/zeolite. Adsorption test was first done with different concentrations of phosphate (5, 10, 15, 20, 25, 30, 35, 40, 45 mg/L) for 12 h at *p*H = 2, 0.04g adsorbent. Nano $Fe(OH)_3$ /zeolite separated from the solution. Then it was immersed in 0.01M $CaCl_2$ solution for another 8 h[46]. After washing and drying, the sorbents were used in the next adsorption-desorption cycle. In order to investigate the regeneration capacity of the nano $Fe(OH)_3$/zeolite adsorbent.

Results and Discussion

Properties of adsorbents

Nanomaterials used as adsorbents were characterized by X-ray diffraction (XRD) (Fig. 1) and scanning electron microscopy (SEM) (Fig.2). Fe NPs produced through chemical reduction appear with some iron oxide (Fe_3O_4) coating (impurity) that possibly was formed in the drying step of the workup. Hence, the XRD patterns for the reduction product show two sets of lines. The first set indicates formation of Fe NPs by showing lines (1 0 0) and (2 0 0), at $2\Theta = 44.82^\circ$ and 65.16°, respectively. The second set designates the Fe_3O_4 impurity, showing

five low intensity lines (2 2 0), (3 1 1), (4 0 0), (5 1 1) and (4 4 0), at 30.17°, 35.53°, 43.38°, 57.13°, and 62.73°, respectively (Fig. 1a). Synthesized nano Fe(OH)$_3$/zeolite was analyzed by XRD. Its zeolite component showed two diffraction peak at 9.45° and 21.98°. In addition, three diffraction peaks at 2Θ = 30.808°, 35.023° and 62.728° with index of (1 1 1), (1 1 1) and (4 4 0) indicated the formation of iron hydroxide (Fig 1b).

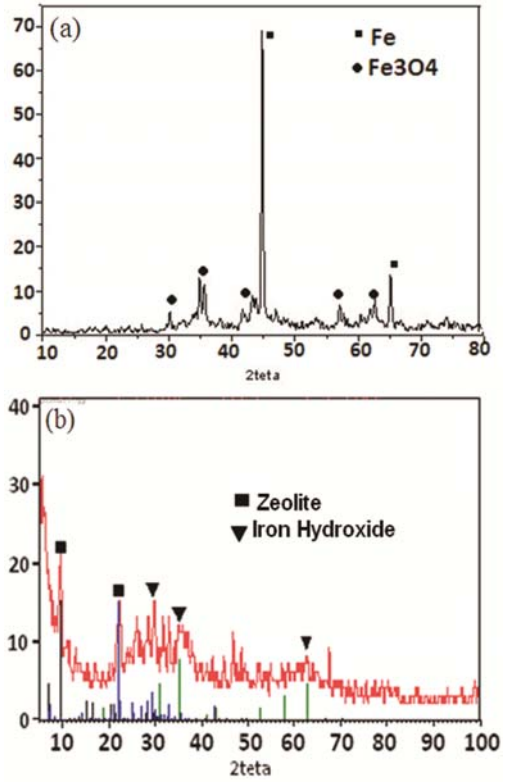

Fig. 1 — XRD patterns of the Fe NPs (a) and nanoFe(OH)$_3$/ zeolite (b).

Using the Scherrer formula[47], diameter of Fe NPs was estimated to be (30 nm). Likewise the mean pore diameter of nano Fe(OH)$_3$/zeolite was found to be 44.2 nm. SEM images indicated that Fe NPs was more clustered than nano Fe(OH)$_3$/zeolite (Fig. 2).

The size and morphology of nanostructured Fe(OH)$_3$/Zeolite was assessed with transmission electron microscopy (TEM) measurement. The TEM images demonstrate that as-formed nanoparticles have size in the range of 25- 50 nm (Fig. 3).

Contact time and sorption kinetics

The results indicated that phosphate removal over our adsorbent sharply increased at the first 8 h and then remained constant for 48 h at 25 ± 1°C. Initially, phosphate removal percentage was slightly higher by Fe NPs than nano Fe(OH)$_3$/Zeolite. Yet, higher removal capacity (83.73%) was gradually achieved by the later, when 15 mg/L initial phosphate concentration was employed. Using zeolite as a stabilizer, prevented agglomeration over time. Previous studies have indicated that, P sorption increases with time[30,32,48]. Thus, depending on the type of material used, sorbent concentration, initial P concentration, equilibrium time may be reached after various times elapsed[49].

The sorption kinetics of phosphorous by nano Fe(OH)$_3$/Zeolite-adsorbent was assessed on the basis of the pseudo-second order kinetic model, according to the Equation. (4)[50]:

$$q_t = \frac{k_2 q_e^{\,2} t}{1 + k_2 q_e t} \quad \ldots (4)$$

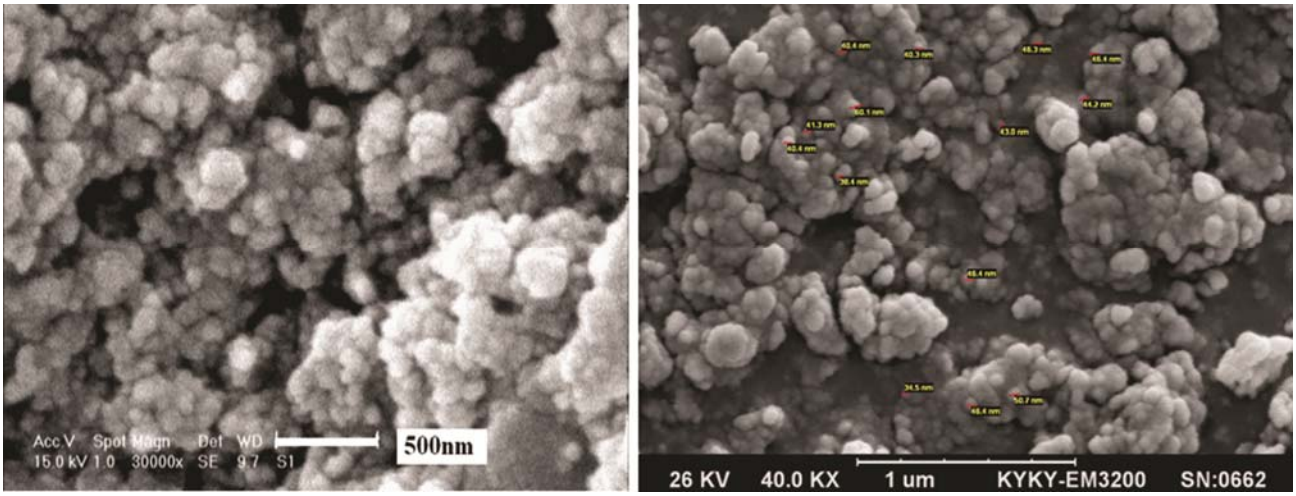

Fig. 2 — SEM images of the Fe NPs (a) and nanoFe(OH)$_3$/zeolite (b).

where t (min) is the contact time, q_t and q_e (mg/g) are the amount of phosphate adsorbed at an arbitrary time t and at equilibrium time, respectively, and k_2 is the rate constant of pseudo-second-order sorption (g $mg^{-1}min^{-1}$). And the pseudo-first order kinetic model, according to the Equation. (5)

$$\ln(q_e - q_t) = -K_1 t + \ln q_e \quad \ldots (5)$$

The pseudo-second order equation fits well with the experimental data, and the correlation coefficients of linear plots obtained for pseudo-second order Equation was 0.9089, for 15 mg/L of initial concentration of P solution (Fig. 4). The k_2 calculated from the slope of Fig. 4 was 0.151g$mg^{-1}h^{-1}$. Furthermore, the sorption capacity calculated by the pseudo-second order model ($q_{e,cal}$, 14.92 mg/g) were close to that determined by the experiment (Table 1). So, it could be concluded that the pseudo-second order kinetic model was better to fit the experimental data and the chemisorption step may be rate determining in the adsorption process[51].

Effects of nanoparticles concentration

The amount of phosphate removal, by our adsorbents, from 40 mL solutions containing varying amounts of initial P, was measured using the following conditions: *p*H = 2, 0.01 M KCl ionic strength, adsorbent amounts of 0.02 or 0.04 g, at 25 ± 1°C. The results indicated that at constant concentration of initial P, its removal percentage increased with higher concentrations of either adsorbent. Nano $Fe(OH)_3$/Zeolite showed a greater removal percentage than Fe NPs, because of using zeolite as its stabilizer which decreased the possibility of aggregation between the nanoparticles. Maximum removal was obtained with 0.04 g nano $Fe(OH)_3$/ Zeolite at 5 mg/L initial concentration of P (*p*H = 2, %90). (Fig. 5a, b). The maximum adsorption capacity by magnetic Fe–Zr binary oxide was 13.65 mg P/g at *p*H = 4[30]. Moharami and Jalali found that the maximum adsorption capacity of P was 28.3, 24.4 and 21.5 mg/g for TiO_2, Fe_3O_4 and Al_2O_3, respectively, with 0.04g of each adsorbent[40]. With 0.2 g Fe-Cu binary oxide, the maximal adsorption capacities for phosphate were 39.8 mg/g at *p*H = 5.0 ± 0.1 and 35.2 mg/g at *p*H = 7.0 ± 0.1, respectively[32].

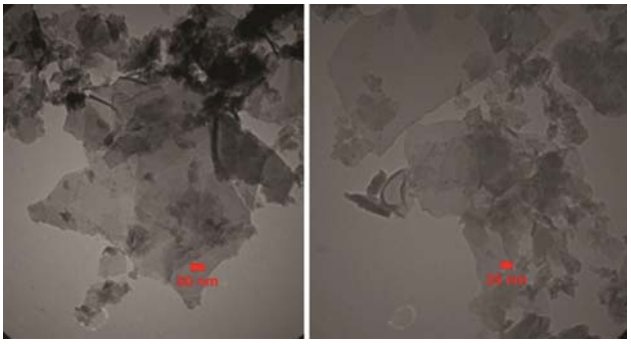

Fig. 3 — TEM images of nano$Fe(OH)_3$/zeolite.

Effects of *p*H on phosphate removal

Remediation of phosphate was measured as a function of *p*H at constant ionic strength (KCl = 0.01 M) for different initial phosphate concentrations (5, 10, 15, 20, 25 mg/L) (Fig. 6, Supplementary information Fig. 1). The removal of phosphate increased as the *p*H decreased. Maximum percentage of P removal could be achieved at *p*H = 2 with 0.04 g adsorbent, possibly in accordance with the following equation (6).

$$Fe(OH)_3 \backslash zeolite + KH_2PO_4\, FePO_4 + 2H_2O + KOH \quad \ldots (6)$$

Studied were carried out on the effects of *p*H on the % phosphate removal by two adsorbents Fe NPs

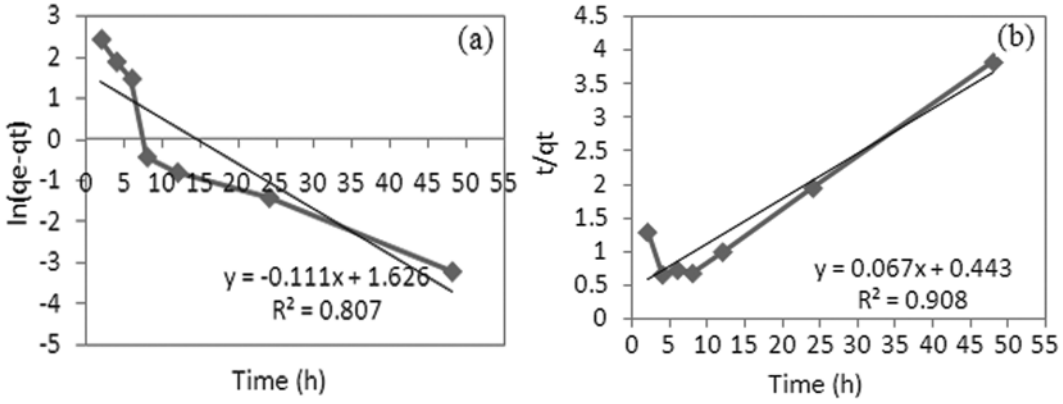

Fig. 4 — Pseudo-first order kinetic model (a) and Pseudo-second order kinetic model (b) of phosphate sorption on the nano $Fe(OH)_3$/zeolite (1 g/L), at 25°C.

Table 1 — The parameters of kinetics models

		Pseudo-first order kinetics			Pseudo-second order kinetics		
Initial concentration (mg l-1)	qe * (mg g-1)	qe ** (mg g-1)	KI (min-1)	R^2	qe ** (mg g-1)	KII (g mg-1 min-1)	R^2
15	12.56	5.062	0.112	0.81	14.92	0.01	0.909

*Experimental data
**Calculated or estimated from the model

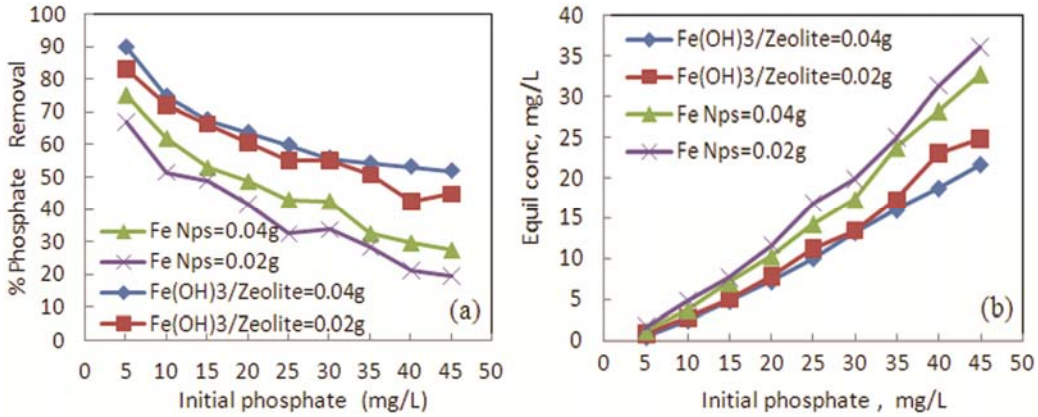

Fig. 5 — Phosphate removal from water (0.01M KCl, *p*H = 2) by two adsorbents FeNPs and nano Fe(OH)$_3$/zeolite each with two concentrations of 0.02 or 0.04 g, after 8 h.

and nano Fe(OH)$_3$/zeolite with the same concentration (0.04 g/ 40 mL), under similar fixed ionic strength (KCl=0.01M), and after equilibrium for 8 h.

Phosphate removal for both cases increased as the *p*H decreased from 8 to 2. A maximum of 90% phosphate removal was demonstrated by nano Fe(OH)$_3$/zeolite. This is in contrast to neat Fe NPs which showed a maximum of 75.2% phosphate removal of phosphate. Nano Fe(OH)$_3$/zeolite showed a greater removal percentage than Fe NPs, because of using zeolite as its stabilizer which decreased the possibility of aggregation between the nanoparticles. Evidently, in acidic condition positive charge builds up on the surface of the adsorbent and hence electrostatic attraction increases anionic adsorption[52]. The above results appear consistent with the following studies. Liu *et al.* described that competition between hydroxyl ions and the phosphate ions on the surface of the adsorbent was the main reason for improving phosphate removal[53]. It can be concluded that, the concentration of hydroxyl ions promoted the opposite reactions described above leading to the decrease of phosphate adsorption at higher *p*H value. Hence the results indicated that the *p*H was a significant parameter controlling the reaction of phosphate removal. In another study Long *et al.* indicated that the Fe–Zr binary oxide could be well used to adsorb phosphate in the acidic environment and adsorption capacity could reach 17.87 mg P/g at *p*H = 3[30]. Lu *et al.* found that the phosphate removal decreased with the increase of *p*H from 3 to 10. At a lower *p*H, the Fe-Ti bimetal oxides surface rendered a rather high phosphate remediation because of the ease of surface protonation (≡M–OH)[31]

Effects of ionic strength on phosphate removal

Studies were carried out on the effects of ionic strength ([KCl] = 0.1, 0.01, or 0.001 M) on phosphate removal by nano Fe(OH)$_3$/Zeolite (0.04 g/ 40 mL), from water, at *p*H = 2, after equilibrium for 8 h (Fig. 7).

Unlike *p*H, the ionic strength had a little influence on the P removal. Another word, for all initial concentrations of phosphate (5, 10, 15, 20, 25 mg/L), not much of difference between P removal was observed, at various ionic strengths. It was stated that Cl^- might be adsorbed by outer sphere association through electrostatic forces, but phosphate could be adsorbed by inner sphere association, showing little sensitivity to ionic strength[54]. Based on this, it might be concluded that phosphate anions could be specifically adsorbed on the two adsorbents (Fe NPs and nano Fe(OH)$_3$/zeolite) *via* forming inner-sphere

surface complexes. In another study workers reached the same results. Long *et al* indicated that a little influence on the removal of phosphate was observed by Fe–Zr binary oxide with different concentrations of ionic strength ([NaCl] = 0.1, 0.01 and 0.001 M)[30]. In the other research, the ionic strength of the solutions varied from 0.001 to 0.1 M by adding different amounts of $NaNO_3$. No significant change was found on phosphate adsorption as a function of increasing ionic strength[32]. Lu *et al.* used 0.001 to 0.1 M NaCl for ionic strength and there was no pronounced influence on phosphate removal for the 2.5 mg/L of phosphate below *p*H 7.0, while a notable effect was observed above that, showing higher phosphate removal with the increasing of ionic strength[31]. Moharami and Jalali found little difference between 0.01M $CaCl_2$ and natural soil solutions when used for ionic strength[40]. This meant that our nano $Fe(OH)_3$/zeolite could be used as an efficient adsorbent for removal of phosphate from high salinity water, with different ionic strength.

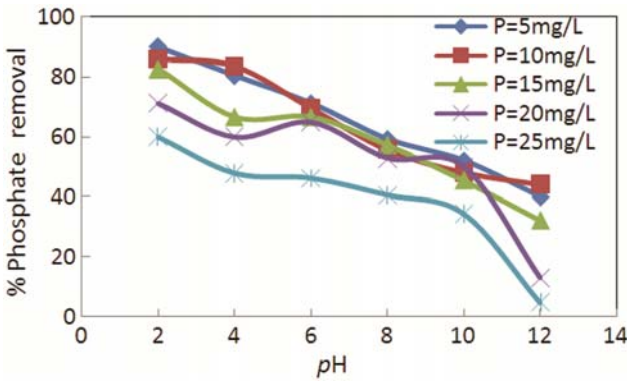

Fig. 6 — Effects of *p*H on the % phosphate removal by nano $Fe(OH)_3$/zeolite (0.04 g/40 mL), KCl = 0.01 M (ionic strength), after equilibrium for 8 h.

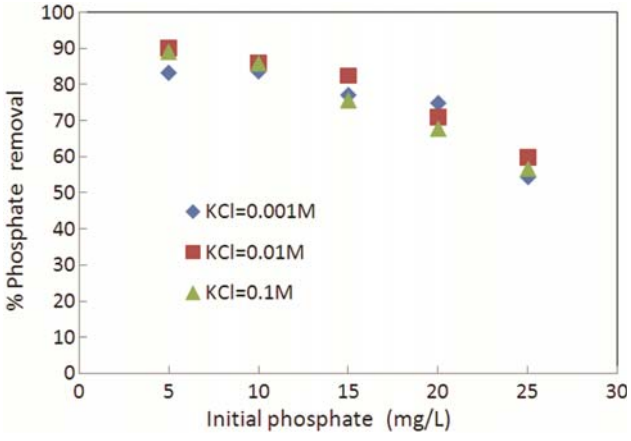

Fig. 7 — Effects of phosphate concentration on its removal by nano $Fe(OH)_3$/zeolite (0.04 g/40 mL), from water with three ionic strengths [KCl]s, at *p*H = 2, after equilibrium for 8 h.

Effects of coexisting anions

Natural water and wastewater always contain lots of coexisting anions, which could potentially compete with phosphate for the adsorption sites. These include anions such as nitrate, bicarbonate, silicate, citrate and acetate that might interfere in the adsorption of phosphate studied in this research (Fig. 8).

The results indicated that the amount of adsorbed phosphate decreased in the presence of nitrate, bicarbonate, silicate and citrate. For bicarbonate and nitrate, only a slight decrease was observed with increasing of their concentrations. Hence these two anions have no significant influence in phosphate adsorption. However, the coexisting silicate decreased the phosphate adsorption. The interference of citrate on phosphate adsorption was much more obvious than others. This may be due to the competition between the phosphate and hydroxyl groups of citrate. The molecular structure of the silicate ion is very similar to the phosphate ion. The obvious inhibition of silicate on phosphate adsorption may be due to the strong competition for the binding sites on the adsorbent between the phosphate and silicate. However, the amount of adsorbed phosphate increased in the presence of acetate which may be caused by the lower final *p*H of sodium acetate solution. It was described above that lower *p*H favored phosphate adsorption. The same results were achieved for ionic competition[30, 32].

Desorption test

Percent phosphate removal was measured after 1-5 cycles. To assess the reusability of the used nano

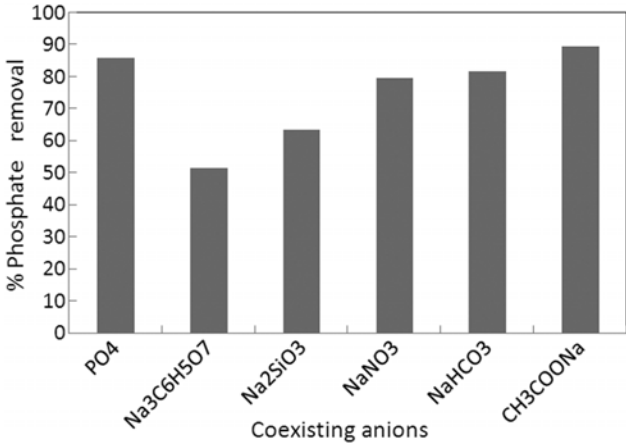

Fig. 8 — Effects of co-existing anions on phosphate adsorption at a fixed initial phosphate concentration (10 mg/L) with an adsorbent dose of (0.04 g/ 40 mL) at *p*H = 2.

Fe(OH)$_3$/zeolite, desorption tests were examined by using $CaCl_2$ 0.01 M. These adsorption-regeneration cycles were carried out up to four times and the results indicated that the phosphate adsorption capacity of the nano Fe(OH)$_3$/zeolite slowly decreased with an increase in the number of regeneration cycle. Hence the adsorption of phosphate on nano Fe(OH)$_3$/ zeolite is relatively reversible and the spent nano Fe(OH)$_3$/ zeolite could be regenerated *via* $CaCl_2$ washing.

Sorption isotherms

One of the key factors required for the design of a sorption system is sorption capacity of adsorbent, which is commonly examined from isotherm data. The sorption percent depends particularly upon the initial adsorbed concentrations. The P removal onto nanoFe(OH)$_3$/zeolite as a function of initial P concentrations (from 5 to 45 mg/L) with two different adsorbent dosage (0.5 and 1 g/L) was studied at constant temperature (298 K) while keeping all other parameters constant (Fig. 9). At the low initial concentration values, P was adsorbed by specific sorption sites, while with increasing initial concentration, the specific sorption sites were saturated and exchange sites were filled. At a low concentration of P (5 mg/L), the amount of P adsorbed onto nano Fe(OH)$_3$/zeolite was 4.5 mg/g. However, at a high P concentration (45 mg/L), the amount of P adsorbed was 23.36 mg/g.

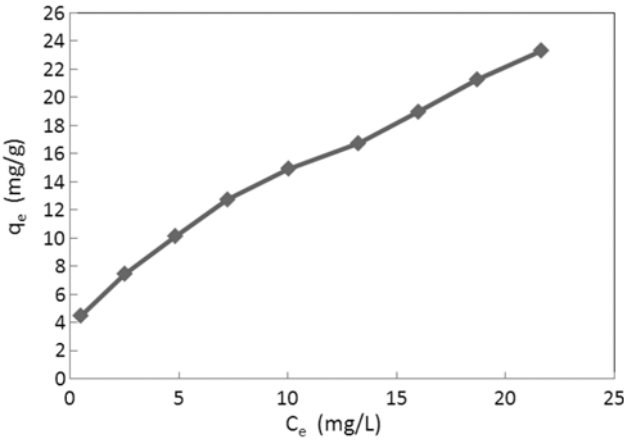

Fig. 9 — Sorption isotherm of phosphate on the nano Fe(OH)$_3$/Zeolite (1 g/L), at 25 °C, after 8 h.

To investigate the sorption mechanism, the corresponding sorption isotherms for P has been quantitatively described by fitting the experimental data to the Freundlich and Langmuir Equations. The Freundlich model is based on the multilayer adsorption of an adsorbate onto the heterogeneous adsorbent surface and its linearized form is expressed by following equation Eq. (7)[55]:

$$q_e = k_F C_e^{1/n} \quad \ldots (7)$$

where K_F is the Freundlich constant that indicates the adsorption capacity and n is an empirical that expresses the adsorption intensity.

The Langmuir model is based on the supposition of surface homogeneity where all the sorption sites are equally available, and with a monolayer surface coverage without interaction between adsorbed species, which could be described by the Eq. (8) as follows[56]:

$$q_e = \frac{K_L q_m C_e}{1 + K_L C_e} \quad \ldots (8)$$

where, q_m (mg/g) is the maximum sorption and K_L(L/mg) is the Langmuir equilibrium constant related to the energy of adsorption and increased with increasing strength of the adsorption bond. Fig. 10 represented the linear plots of Langmuir and Freundlich Equations of phosphorous adsorption, and

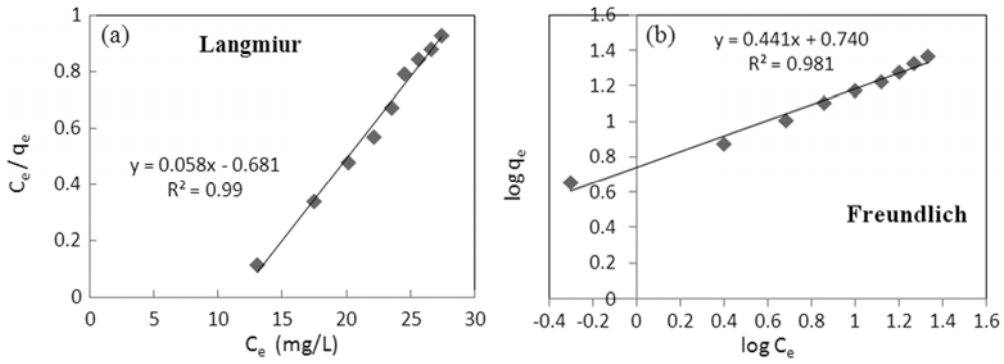

Fig. 10 — The linear fitting of Langmuir (a) and Freundlich theory (b) sorption isotherms of phosphate on the nano Fe(OH)$_3$/zeolite (1 g/L), at 25 °C, after 8 h.

Table 2 — Isotherm constants for the sorption of phosphate onto nano $Fe(OH)_3$/zeolite -adsorbent at 298 K

Freundlich model parameters			Langmuir model parameters			
R^2	$1/n$	K_F	R_L	R^2	K_L	q_{max}
0.9818	0.4419	5.91	0.21–0.69	0.99	0.0859	17.065

the sorption constants of fitted models parameters and correlation coefficients (R^2) were calculated and illustrated in Table 2.

Based on R^2 values which displayed the applicability of a particular isotherm model, the Langmuir model was fitted with the sorption data better than the Freundlich model. This result was in consistent with the previous studies that showed the Langmuir isotherm was the most popular to explain P sorption[57].

Additionally, the degree of suitability of adsorbent towards adsorbates is assessed from the values of separation factor constant (R_L) through following Equation. (9)[58]:

$$R_L = \frac{1}{1 + K_L C_0} \quad \text{... (9)}$$

The value of R_L depicts the monolayer adsorption predicted by the Langmuir model is irreversible (R_L = 0), favorable (0 <R_L< 1), linear (R_L= 1), or unfavorable (R_L> 1). The calculated values of R_L (Table. 2) indicated that the adsorption was favorable as the R_L values were calculated between 0 and 1.

Conclusion

Both nanoparticles could be used for phosphate removal from water. This is mostly due to chemical absorption process between Fe and phosphate in the acidic environment by ion exchange and surface adsorption in acidic condition. However, aggregation that occurs during the reaction may reduce the reactive surface area. This was somewhat eliminated by coating Fe nanoparticles on a zeolite stabilizer, which enhanced phosphate removal by 30% and greatly improved phosphate remediation from 53% to 83% at *p*H = 2, with initial P concentrations of 15 mg/L. This improvement is attributed to a better reaction of Fe with phosphate by increasing nano particles effective surface area. Moreover, replacement of the hydroxyl ion with phosphate is also helped. The removal of phosphate increase with decreasing *p*H. The maximal adsorption capacities for phosphate are 90% at *p*H 2.0 ± 0.1 by nano $Fe(OH)_3$/zeolite and 75% at *p*H 2.0 ± 0.1 by Fe NPs. Kinetic studies on the phosphate removal from water with $Fe(OH)_3$/zeolite nano adsorbent show that 8 h is nearly enough to achieve the sorption equilibration and sorption kinetic agreed well with pseudo-second order model. Furthermore, the sorption isotherm fitted well to the Langmuir model and the maximum sorption capacity is found to be 17.065 mg/g. It may be concluded that nano iron hydroxide particles modified by zeolite can effectively be used for phosphate removal from water resources because of the increase in its reactive surface area and therefore the higher efficiency in p removal. Moreover zeolites could maintain phosphate with their porous structure. The phosphate-loaded nano $Fe(OH)_3$/zeolite could be effectively regenerated by 0.01 M $CaCl_2$ and reused for the phosphate adsorption for several times. This adsorbent might be a promising one for the removal of phosphate from aqueous solutions. With respect to the importance of this research in human health, it is recommended to evaluate this technique in a large scale.

References

1 Lin L, Lei Z, Wang L, Liu X, Zhang Y, Wan C, Lee D J & Tay J H, *Sep Pur Technol*, 103 (2013) 15.
2 FAO, (Food And Agriculture Organization Of the United Nations, Rome), 2012.
3 Lin J, Zhan Y & Zhu Z, *Sci Total Environ*, 409 (2011) 638.
4 Blancy L M & Cinar S, *Water Res*, 41 (2007) 1603.
5 Salome G P & Soares E J, *Catal Lett*, 126 (2008) 253.
6 Dupas R, Delmas M, Dorioz J M, Garnier J, Moatar F & Gascuel Odoux C, *Ecol Indicators*, 48 (2015) 396.
7 Kalff J, Limnology, (Inland Water Ecosystems. Prentice Hall, Upper Saddle River), 2002.
8 Lewis W M, Wurtsbaugh W A & Paerl H W, *Environ Sci Technol*, 45 (2011)10300.
9 Ma L, Velth of G L, Wang F H, Qin W, Zhang W F, Liu Z, Zhang Y, Wei J, Lesschen J P, Ma W Q, Oenema O & Zhang F S, *Sci Total Environ*, 434 (2012) 51.
10 Strokal M, Yang H, Zhang Y, Kroeze C, Li L, Luan S, Wang H, Yang S & Zhang Y, *Mar Pollut Bull*, 85 (2014) 123.
11 Bechmann M B, Berge D, Eggestad H O & Vandsem S M, *J Hydr*, 304(2005) 238.
12 Grizzetti B, Bouraoui F & Aloe A, *Global Change Biol*, 18 (2012) 769.
13 Puijenbroek P J, Van T M, Cleij P & Visser H, Ecol Indic, 36 (2014) 456.
14 Taghipour M & Jalali M, J Hazard Mater, 283 (2015) 359.
15 Windolf J, Blicher Mathiesen G, Carstensen J & Kronvang B, Environ Sci Polic, 24 (2012) 24.
16 Yang Z C, Zhao N, Huang F & Lv Y Z, Soil Till Res, 146, Part A, (2015) 47.
17 Jalali M, Environ Geol, 57 (2009) 1011.

18 Roberts T L, Procedia Eng, 83 (2014) 52.
19 Bennion H, Juggins S, Anderson N J, Environ Sci Technol, 30 (1996) 2004.
20 Chapra S C, (Surface Water-Quality Modeling, Singapore, McGraw-Hill Inc), 1997.
21 Park J K, Wang J &Novotny G, (Department of Natural Resources), 174 (1997).
22 Zhao Y, Wang J, Luan Z, Peng X, Liang Z & Shi L, *J Hazard Mater*, 165 (2009) 1193.
23 Bekta N, Akbulut H, Inan H & Dimoglo A, *J Hazard Mater*, 106 (2004) 101.
24 Zhang W X, *J Nanopart Res*, 5 (2003) 323.
25 Qu X, Alvarez P J J, Li Q, *Water Res*, 47 (2013) 3931.
26 O' Carroll D, Brent S, Magdalena K, Hardilieet B & Christopher K, *Adv Water Resour*, 51 (2013) 104.
27 Tosco T, Papini M P, Viggi C C & Sethi A, *J Clean Product*, 77 (2014) 10.
28 Cumbal L, Greenleaf J, Leun D & Sen Gupta A K, *React Funct Polym*, 54 (2003) 167.
29 Nurmi J T, Tratnyek P G, Sarathy V, Baer D R, Amonette J E & Pecher K, *Environ Sci Technol*, 39 (2005) 1221.
30 Long F, Gong J L, Zeng G M, Chen L, Wang X Y, Deng J H, Niu Q Y, Zhang H Y &Zhang X R, *Chem Eng J*, 171 (2011) 448.
31 Lu J, Liu D, Hao J, Zhang G & Lu B, *Chem Eng Res Des*, 93(2015) 652.
32 Li G, Gao S, Zhang G & Zhang X, *Chem Eng J*, 235 (2014) 124.
33 Lin C J, Lo S L & Liou Y H, *Chemosphere*, 59 (2005) 1299.
34 Liou Y H, Lo S L, Lin C J & Kuan W H, *Water Res*, 41 (2007) 1705.
35 Lee C C & Doong R A, *Environ Sci Tech*, 42 (2008) 4752.
36 Zhu H J, Jia Y F, Wu X &Wang H, *J Hazard Mater*, 172 (2009) 1591.
37 An B & Zhao D, *J Hazard Mater*, 211 (2012) 332.
38 Motamedi E, Talebi Atouei M & Kassaee M Z, *Mater Res Bull*, 54 (2014) 34.
39 Gan L, Zuo J, Xie B, Li P & Huang X, *J Environ Sci*, 24 (2012) 1929.
40 Moharami S & Jalali M, *Environ Prog & Sustainable Energ*, (2014) (Vol.00, No.00).
41 Liu F, Yang J H, Zuo J, Ma D, Gan L, Xie B, Wang P & Yang B, *J Environ Sci*, 26 (2014) 1751.
42 Huang Y, Yang J K & Keller A A, *ACS Sustainable Chem Eng*, 2 (2014) 1128.
43 Saad R, Thiboutot S, Ampleman G, Dashan W & Hawar J, *Chemosphere*, 81 (2010) 853.
44 Valle Orta M, Diaz D, Santiago Jacinto P, Vazquez Olmos A & Reguera E, *J Phys Chem*, 112 (2008) 14427.
45 Kassaee M Z, Motamedi E, Mikhak A & Rahnemaie R, *Chem Eng J*, 166 (2011) 490.
46 Auxtero E, Madeira M & Sousa E, *Geoderma*, 144 (2008) 535.
47 Birks L S & Friedman H, *J Appl Phys*, 16 (1946) 687.
48 Violante A & Pigna M, *Soil Sci Am J*, 66 (2002) 1788.
49 Cucarella V & Renman G, *J Environ Qual*, 38 (2009) 381.
50 Ho Y S & McKay G, *Process Biochem*, 34 (1999) 451.
51 Fornasiero P, Kašpar J & Graziani M, *Appl Catal B*, 22 (1999) L11.
52 Palanisamy P N & Sivakumar P, *Desalin*, 249 (2009) 388.
53 Liu H L, Sun X F, Yin C Q & Hu C, *J Hazard Mater*, 151 (2008) 616.
54 McBride M B, *Clay Clay Miner*, 45 (1997) 598.
55 Freundlich H, *Phys Chem Soc*, 40 (1906) 1361.
56 Langmuir I, *J Am Chem Soc*, 40 (1918) 1361.
57 Xu D, Xu J, Wu J & Muhammad A, *Chemosphere*, 63 (2006):344.
58 Hao Y M, Man C & Hu Z B, *J Hazard Mater*, 184 (2010) 392.